Methods for controlling positions of guided modes of photonic-crystal waveguides

Marko Lončar, Jelena Vučković, and Axel Scherer

Department of Electrical Engineering, California Institute of Technology, EE 136-93, Pasadena, California 91125

Received December 6, 2000; revised manuscript received March 23, 2001

We analyze different methods for controlling positions of guided modes of planar photonic-crystal waveguides. Methods based both on rearrangements of holes in the photonic-crystal lattice and on changes of hole sizes are presented. The ability to tune frequencies of guided modes within a frequency bandgap is necessary to achieve efficient guiding of light within a waveguide, as well as to match frequencies of eigenmodes of different photonic-crystal-based devices for the purpose of good coupling between them. We observe and explain the appearance of acceptor-type modes in donor-type waveguides. © 2001 Optical Society of America

OCIS codes: 250.0250, 000.4430, 230.7390, 230.3990, 250.5300.

1. INTRODUCTION

The generation, guiding, and detection of lightwave signals are fundamental tasks in any optical system. Ideally, to make small-scale all-optical signal-processing devices, it is necessary to have the components that are doing each of these tasks integrated on one chip. Photonic crystals[1,2] (PCs) introduced in recent years are thought to be promising candidates for achieving this high level of integration. Owing to the difficulties associated with the fabrication of three-dimensional (3D) photonic crystals, planar photonic crystals[3] (PPCs) have attracted significant research attention. The basis of the PPC is a dielectric slab, perforated with a two-dimensional (2D) periodic lattice of holes. The symmetry of the lattice (triangular, square, etc.) plays a crucial role and determines properties of the PPC.[2,4] Due to the periodicity of the lattice, frequency bandgaps for guided modes of the slab are opened, and light of certain frequencies cannot propagate in the slab. The light is localized to the slab in the vertical direction by means of total internal reflection and is controlled in the lateral direction by the 2D PC. The combination of these two mechanisms makes localization of light in all three dimensions possible.

PC waveguides have attracted a lot of attention since they were proposed for the first time.[5] The most interesting property of the PC waveguide is the possibility of making sharp bends with acceptable transmission efficiency around the bend.[6,7] So far, many groups have investigated different properties of PC waveguides.[8–12] In most of these studies, waveguides were defined as single-line or multiline defects in the PC lattice, formed by removing one or more rows of holes. Modal analysis of these types of waveguides show that they are multimode. Recently, Adibi *et al.*[13] have proposed and analyzed in 2D a novel way of reducing the number of modes in the waveguide. Experimental characterization of guiding in PC waveguides was also reported by several groups.[14–17]

In this paper we investigate different waveguide designs, based on a triangular PPC lattice, and investigate their properties by analyzing ω–β dispersion relations. We show several ways of controlling the frequencies of guided modes, a feature that can also lead to the single-mode regime of operation of the waveguide. The ability to control positions of guided modes within a frequency bandgap of the surrounding PPC is necessary for achieving three important goals: efficient guiding of light (reduced lateral and vertical losses), efficient coupling of light from an external light source into the waveguide (no leaky modes at the frequency of interest), and efficient coupling of different PC devices (for example, frequency matching of eigenmodes of a cavity and a waveguide coupled to it).

All the structures presented in this paper are fabricated of silicon. Details on the fabrication procedure are presented in our previous paper.[10]

2. METHOD OF ANALYSIS

The waveguides described here were analyzed with the finite-difference time-domain (FDTD) method.[18] We analyzed Si slabs (refractive index assumed to be $n_{\mathrm{Si}} = 3.5$) of thickness $t = 0.55a$, surrounded by air on both sides, and perforated with a 2D triangular lattice of holes of radius $r = 0.3a$ (Fig. 1). Parameter a is the periodicity of the lattice. The discretization of the space used in 3D FDTD code was $a = 20$ computational points. In all analyses that follow we analyze only one half of the structure in the vertical direction, with a mirror boundary condition (BC) applied at the middle of the slab. In that way we could select between vertically even (TE-like) and vertically odd (TM-like) modes. As it has been shown before, in this structure a bandgap exists for TE-like guided modes only. Another motivation for using the mirror BC in the middle of the slab was a substantial reduction of time necessary for performing the calculations. In the vertical direction we apply Mur's absorbing boundary conditions (ABCs) at the distance of $4a$ points from the surface of the slab. In the y direction we apply Bloch boundary conditions (BCs), and in that way we can control the propagation constant of the mode (β). In the x direction

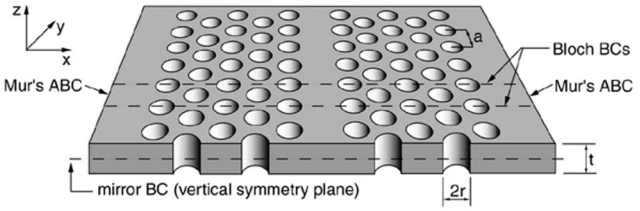

Fig. 1. Schematic of the single-line defect waveguide. Unit-cell and boundary conditions used in the FDTD calculation are indicated.

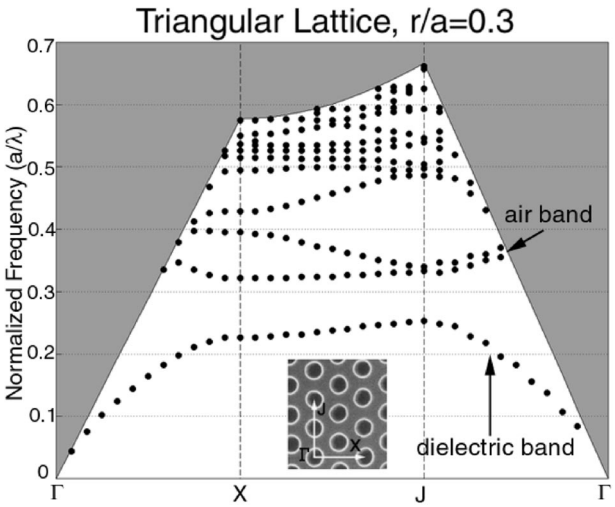

Fig. 2. Band diagram for the TE-like (vertically even) modes of the Si slab perforated with a triangular lattice of air holes. Parameters used in the analysis are $r = 0.3a$ (hole radius), $t = 0.55a$ (slab thickness), and $n_{Si} = 3.5$ (refractive index of Si).

we apply Mur's ABC after eight layers of PC at both sides of the waveguide. The FDTD method used to find the dispersion relations is as follows[19]: We use some initial field distribution in the waveguide (Gaussian in our case) and then evolve the field in time using the BCs described above. We store the field components in several low-symmetry points in the waveguide, and then we find the spectrum of that time evolution. The peaks in the spectrum correspond to the eigenmodes of the structure. To obtain the dispersion diagram, we plot the dependence of the frequencies of the eigenmodes versus the propagation constant. In this paper we are concerned mostly with TE-like modes, although TM-like modes can also be guided due to the effective refractive-index contrast between the line of missing holes and the perforated slab, as shown in our previous study.[10]

The first step in analysis of any PC-based device is calculation of the band diagram. We used a method similar to the one described above to analyze a unit cell of a triangular lattice by applying appropriate boundary conditions: Bloch BCs at all four sides of the cell in the lateral direction, a mirror BC at the middle of the Si slab, and the Mur's ABC after $4a$ points from the top surface of the slab. As it was mentioned above, the geometry used was $r/a = 0.3$. In previous research[10] we used the value $r/a = 0.4$. The smaller value of r results in a narrower bandgap but in turn improves localization of light within a slab, which is especially important for efficient turning of corners. Also, in the case of a dielectric membrane suspended in air, the structure with smaller holes is mechanically more stable. Figure 2 shows the band diagram for the guided modes of the Si slab perforated with the 2D lattice of holes, for $r/a = 0.3$. The bandgap for the guided modes of the perforated dielectric slab is open around the normalized frequency of $a/\lambda_0 = \omega a/2\pi c \approx 0.28$.

3. SINGLE-LINE DEFECT WAVEGUIDE

By omitting one row of holes we can form a simplest waveguide (type 0), shown in Fig. 1. The localization of light within the line defect can be explained in the following way: by omitting one row of holes we are adding more high-refractive-index material, and therefore frequencies of some modes from the air band are reduced and they are pulled down into the bandgap to form localized defect states. This type of waveguide, in which we increase the amount of the high-dielectric material in comparison with the unperturbed PPC, will be called a donor-type waveguide. Propagation of light in the lateral direction is suspended since the defect mode of the waveguide is within the frequency bandgap of the PPC, and, in the vertical direction, because of the refractive-index contrast of the Si slab and the surrounding air (total internal reflection).

Figure 3(a) shows the dispersion diagram for guided modes of a single-line defect waveguide. The modes above the light line will leak energy into the air (leaky modes). The crossing of mode 1 and mode 2 in Fig. 3 is due to the different symmetry properties of these two modes in the lateral direction. Mode 1 is odd and mode 2 is even with respect to the mirror plane in the center of the waveguide. In this paper we are interested only in truly photonic-bandgap guided modes of the waveguide. Therefore from here on (Figs. 5, 8, and 9) we show only those modes that are located in the frequency bandgap. (For a general discussion on different guiding mechanisms in this type of waveguide, the interested reader is directed to our previous research[10]). Furthermore, modes 3 and 4 are not of any practical interest since they are located close to the band edge and therefore are pushed back into the air band as we make some changes to the waveguide. Because of that, they are not included in the analysis that follows. In this paper we are interested in the position of the modes 1 and 2 and any other additional modes that appear as we make some changes to the single-line defect waveguide.

For comparison, in Fig. 3(b) we show the dispersion diagram for modes guided in a single-line defect waveguide with $r/a = 0.4$, where all other parameters are held the same as in Fig. 3(a). It is important to notice mini stop bands open for $\beta = \pi/a$ (the Brillouin zone boundary) and for $\beta = 0$ [Fig. 3(b)]. These mini stop bands were not observed in our past study[10] due to insufficient frequency resolution used in those calculations. In the present study we use the same method of analysis but run the simulations for considerably longer periods of time in order to improve the frequency resolution. It is clear that the structure with larger holes has a much

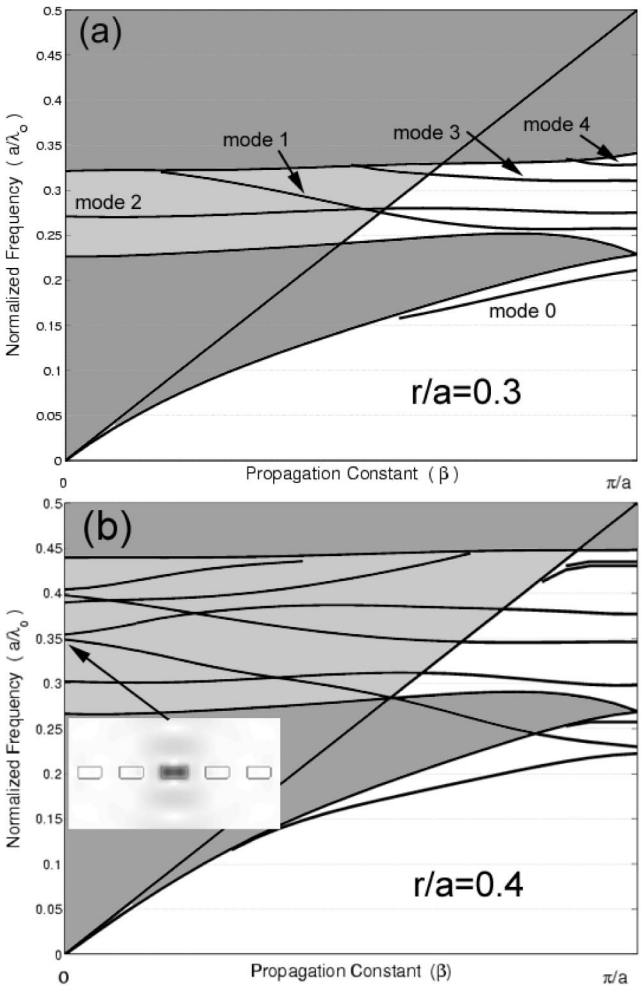

Fig. 3. ω–β relation for the guided modes in the single-line defect waveguide (type 0) for (a) $r/a = 0.3$ and (b) $r/a = 0.4$. The inset shows the amplitude of the E field (cross section) in the case of one leaky mode. The straight solid line represents the light line. Modes above the light line, in the light-gray region, will leak energy into the air (leaky modes). Dark gray areas are the regions in which extended states of the PPC slab exist. Guiding can occur in the white regions only.

more complicated dispersion diagram. The most important difference between the two structures is that in the case of bigger holes, leaky modes exist at all bandgap frequencies [inset in Fig. 3(b)]. Therefore by coupling light from an external light source into the waveguide, leaky modes are excited as well, and the coupling efficiency decreases. This could explain vertical losses observed in Ref. 16. On the other hand, in the structure with $r/a = 0.3$ there are no leaky modes in the frequency range in which mode 1 becomes guided [Fig. 3(a)]. However, mode 1 is not very well confined to the waveguide and decays slowly into the PPC, since it is located close to the dielectric-band edge. Thus it may suffer from the finite-size effects of PPC and may be more sensitive to the fabrication disorder. To achieve efficient guiding of light, it is possible to push mode 1 to higher frequencies, closer to the midgap, and to use it as our guided mode of preference. This can be achieved by reducing the amount of high dielectric material that forms the waveguide.

Before analyzing different methods of controlling positions of guided modes, it is important to notice that all photonic-bandgap guided modes in Fig. 3 (below the light line, and in the frequency bandgap) have an almost flat dispersion relation. Therefore these modes will have small group velocities and will be able to guide light only in a very narrow frequency range. This is very different from an ideal case, where we want to have an efficient transport of energy in a wide frequency range. Also, coupling between PC waveguides and plain ridge waveguides is expected to be poor due to different dispersion characteristics of the two waveguides, and alternative methods of adiabatic coupling need to be investigated.[20]

4. DIFFERENT METHODS FOR CONTROLLING POSITIONS OF THE GUIDED MODES

A. Methods Based on Rearrangements of PPC Lattice

A straightforward way of controlling frequencies of the guided modes is reduction of the waveguide width. This can be achieved by moving the two PPC mirrors that surround the single-line defect toward one another along the ΓX direction [Figs. 4(a) and 4(b)]. We call this type of waveguide type 1. Similar structure has been previously analyzed in two dimensions by Benisty *et al.*[21] We performed full 3D FDTD analysis of the structure. The dispersion diagram of the guided modes in waveguides of different widths is shown in Fig. 5(a). We can observe that modes 1 and 2 are shifted toward higher frequencies as the width of the waveguide decreases. For parameter $M = 5$, mode 1 is shifted closer to the midgap frequency, and therefore losses related to the leaks into the PPC are reduced. This means that mode 1 can be used to guide the light in the waveguide. However, a big disadvantage of a type 1 waveguide is the broken symmetry of the triangular lattice; it is impossible to create sharp bends with the waveguide sections of the same width [Fig. 4(b)] un-

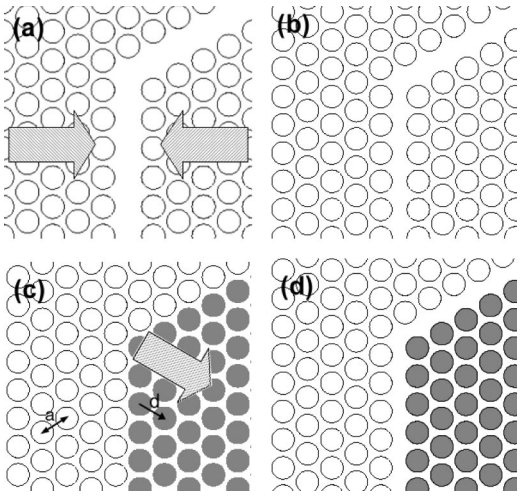

Fig. 4. Different types of waveguides. By moving PPC mirrors that surround (a) a single-line defect waveguide along the direction indicated by arrows (ΓX direction) we can form (b) a type 1 waveguide. (c) Unperturbed PPC lattice. If we offset the gray holes along the ΓJ direction for amount d, we can form (d) a new type of waveguide (type 2). By controlling the parameter d, we can control the positions of the guided modes of the structure.

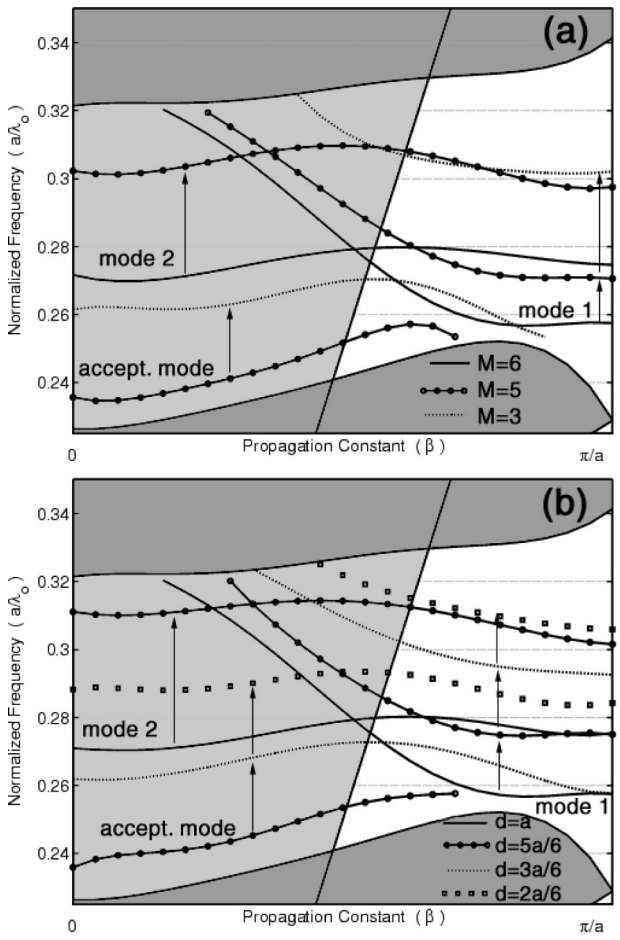

Fig. 5. Dispersion relations for the guided modes of the type 1 and type 2 waveguides for different values of controlling parameters, M and d, respectively. Arrows indicate positions of the modes as we change the controlling parameters. (a) Type 1 waveguide. The width of the waveguide (center-to-center distance between two holes adjacent to the waveguide) is defined as $a\sqrt{3}/2(1 + M/6)$. $M = 6$ yields single-line defect waveguide. (b) Type 2 waveguide. Position of the modes as a function of the parameter d, offset along the ΓJ direction.

less we create unwanted line defects close to the bend and in that way reduce the bending efficiency.

Another, more promising, method of controlling positions of guided modes is shown in Fig. 4(d). This type of waveguide is called type 2. The waveguide is formed from the PPC lattice by moving two regions of PPC apart, along the ΓJ (nearest-neighbor) direction, by the offset $d = la$ [Figs. 4(c) and 4(d)], where l is a real number. For $l = 1$ we can form the single-line defect waveguide, and for $0 < l < 1$ we can form a waveguide narrower than a single-line defect. In this structure it is possible to create sharp 60° bends within the waveguide without introducing unwanted line defects [Fig. 4(d)]. Dispersion characteristics for guided modes in this waveguide, as a function of the parameter d, are shown in Fig. 5(b). For $d = 0.5a$, mode 1 is pushed to around the midgap frequency, and mode 2 is pushed out of the bandgap, all the way back into the air band. Therefore we achieve our goals of designing a waveguide with reduced lateral losses (due to the finite-size effects and fabrication disorder) and increased coupling efficiency, since there are no leaky modes at the frequency of interest. However, because of the dislocation of the PPC regions, creation of 120° bends as well as an easy integration of a type 2 waveguide with PC cavities is not straightforward.

This method of creating waveguides is not limited to a triangular-lattice PPC. For example, by off-setting holes along the second-nearest-neighbor direction in a square-lattice PPC, we can form the waveguide narrower than a single-line defect and still be able to form 90° bends within it.

There is one interesting feature that can be observed in Fig. 5(b). An extra mode, pulled from the dielectric band up into the bandgap, appears as we reduce the value of the parameter d. This mode, labeled "accept. mode" in Fig. 5(b), has the same symmetry as mode 1, and therefore the two modes interact strongly (anticrossing). This mode can be also observed in the case of the type 1 waveguide [Fig. 5(a)]. Now, it has to be explained why the acceptor-type guided modes appear in the donor-type waveguide, since we would expect that, by adding dielectric material, only donor-type guided modes are excited. To explain this, we focus our attention on Fig. 6. Figures 6(a) and 6(b) show amplitudes of the electric field in the unperturbed PPC (at the X point) in the case of a dielectric and an air band, respectively. In Fig. 6(c), unperturbed PPC is represented by the black holes on the left-hand side and the open holes on the right-hand-side of the figure. The offsetting of the open holes by amount $d = a$ in the ΓJ direction is equivalent to the removal of one row of holes: the net result is a single-line defect waveguide (type 0). In either case there are regions in which dielectric substitutes for air, and therefore modes from the air band are pulled down into the bandgap to form localized states. However, if the offset is less than a, for example, $d = 0.5a$ in the case of Fig. 6(c) (new po-

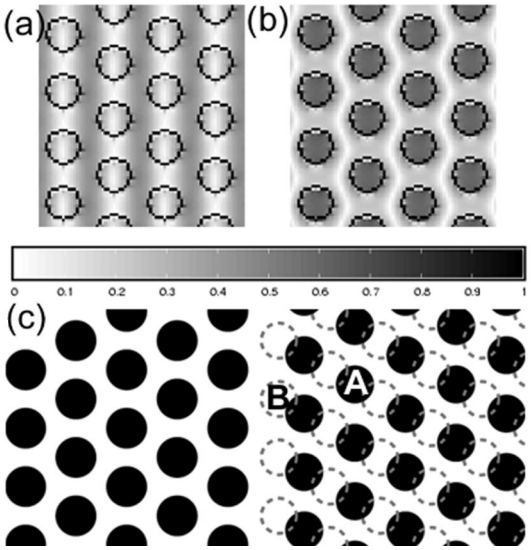

Fig. 6. Amplitude of the electric field at the X point in the unperturbed PPC in the case of (a) the dielectric and (b) the air bands. The intensity bar is also shown. (c) A type 2 waveguide for $d = 0.5a$ (black holes). The regions in which air replaces dielectric (A) and vice versa (B) as we move holes around are also indicated. Black holes on the left-hand side and open holes on the right-hand side represent positions of the holes in the unperturbed PPC.

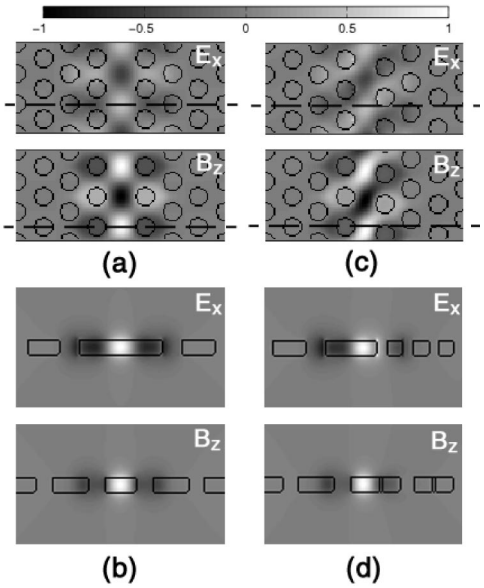

Fig. 7. (a), (b) Field pattern of mode 1 in the type 1 waveguide for $M = 5$. (c), (d) Field pattern of mode 1 in the type 2 waveguide, for $d = 0.5a$. (a) and (c) show field profiles at the middle of the slab, and (b) and (d) show field profiles at the positions indicated by dashed lines in (a) and (c), respectively. An intensity bar is also shown. Field patterns are shown for $\beta = \pi/a$.

sitions of the holes are represented by the black circles on the right-hand side), there will be regions in which air appears instead of the dielectric (A), in addition to regions in which dielectric replaces the air (B). Therefore modes from the dielectric band one pulled up into the bandgap, due to their increased overlap with air (acceptor-type modes) and modes from the air band are pulled down into the bandgap due to increased overlap with the dielectric (donor-type modes). This explains the appearance of both types of modes in a donor-type waveguide. Therefore we conclude that, to form the waveguide, what matters is not the absolute amount of the dielectric material added to the PPC but rather the relative position of the holes in the unperturbed and the perturbed PPC.

In Fig. 7 we show field patterns of mode 1 in the case of type 1 and type 2 waveguides, for parameters $M = 5$ and $d = 0.5a$, respectively. In both cases, E_x and B_z fields have antinodes at the middle of the waveguide, and therefore it is possible to efficiently couple TE-polarized light from an external light source into the waveguide.

B. Methods Based on Changes of the Size of Holes

So far we have investigated properties of three different types of waveguides. In all cases, waveguides were formed as narrow regions of high-dielectric-constant material, surrounded by the PPC mirrors at both sides. The positions of the guided modes were then controlled by moving the holes around. Besides this approach, positions of guided modes can also be controlled by changing the size of the holes in one or more rows. For example, if we increase the radius of the holes adjacent to the single-line defect waveguide, we can form a new type of waveguide: type 3 [Fig. 8(a)]. This method was proposed and analyzed in two-dimensions by Adibi *et al.*[13] Here, we present results of the 3D FDTD analysis of the structure.

In Figs. 8(b) and 8(c) we show the dispersion relation for the TE-like guided modes in this waveguide. As expected, by increasing the size of the holes, the modes of the original waveguide (type 0) are shifted toward higher frequencies, indicated by arrows. Also other modes, in both laterally even and odd cases, appear; these are acceptor-type modes, pulled up from the dielectric band due to the increased size of the holes adjacent to the waveguide. This is particularly dramatic in the case of the laterally odd modes, in which the acceptor-type mode interacts strongly with the donor-type mode 1, and the two anticross. Therefore the feature observed in the study by Adibi *et al.*,[13] the bending of mode 1, is due to its interaction with the acceptor-type mode. For $r_{\mathrm{defect}}/a = 0.5$, all the donor-type guided modes are pushed back into the air band (there are some leaky donor-type modes, though), and the only modes that remain are the acceptor-type modes.

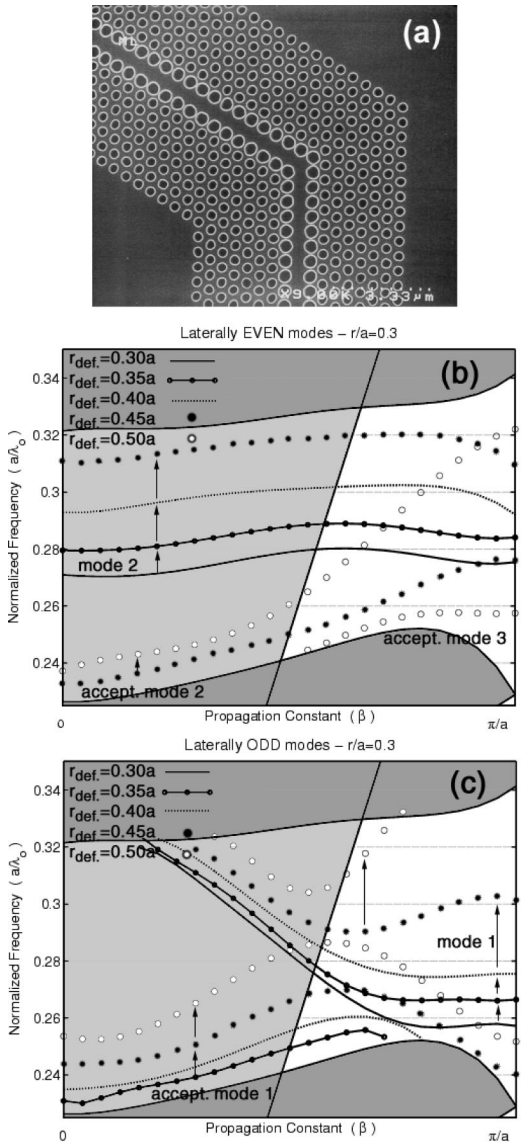

Fig. 8. (a) Scanning electron microscopy micrograph of the fabricated type 3 waveguide. Dispersion relations of (b) the laterally even and (c) the laterally odd modes as a function of the size of the holes adjacent to the waveguide.

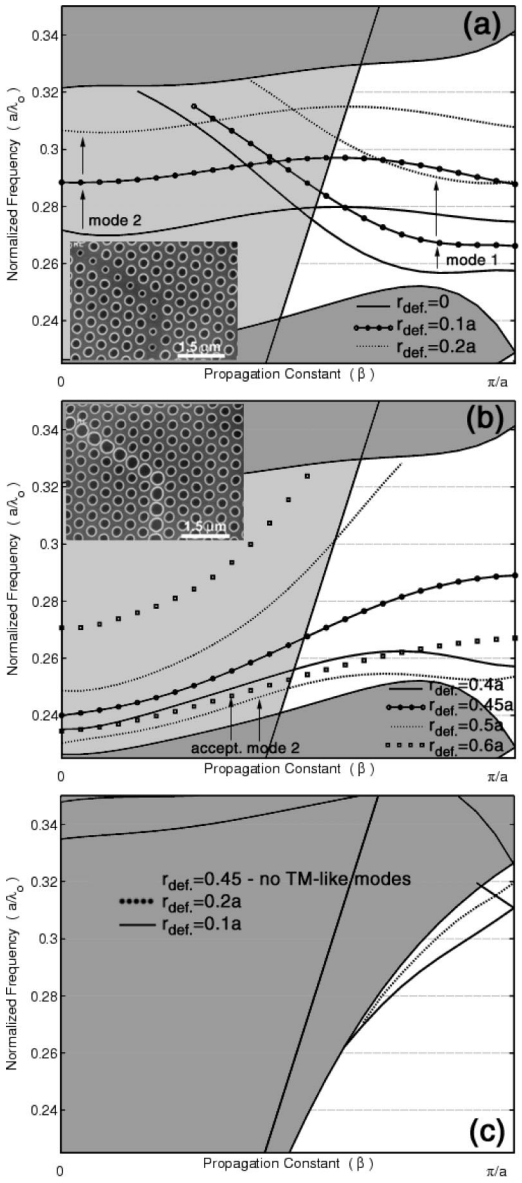

Fig. 9. Dispersion relations for the modes guided in (a) the type 4 and (b) the type 5 waveguides, as a function of the radius of the defect holes (r_{defect}). Arrows indicate positions of the modes for different values of r_{defect}. Scanning electron microscopy micrographs of the fabricated structures are shown in the insets. (c) Dispersion diagram for TM-like guided modes supported in type 4 and type 5 waveguides.

In conclusion, this waveguide has a rather complicated band structure, and many modes are present because we have changed the properties of three rows of holes. Therefore it is probably not a good candidate for efficient control of positions of the modes within the bandgap. Also we expect this waveguide to have reduced transmission efficiency around sharp corners due to the increased vertical losses at the corner, as a result of enlarged holes. The advantage of this structure over the type 1 and type 2 waveguides is that no holes are moved, and therefore the structure has the same symmetry as the type 0 waveguide. Because of that, it is possible to create not only the 60° bends but also the 120° ones.

Another promising mechanism of controlling positions of guided modes within a bandgap is shown in insets in Figs. 9(a) and 9(b). The waveguide is formed by reducing (donor-type) or increasing (acceptor-type) the radii of holes in one row. (During the process of writing this paper, another group has published results of the analysis of the guided modes in similar structures.[9] However, our analysis includes the leaky modes as well, since they are important for determining the efficiency of waveguide operation at the desired frequency.)

In Fig. 9(a) we can observe that by reducing the size of the holes from $0.3a$ to 0, modes move toward lower frequencies. For $r_{\text{defect}} = 0.2a$ (small perturbation to the rest of PPC with $r = 0.3a$) mode 1 is centered around the midgap frequency. In addition, coupling from an external light source is good since there are no leaky modes around the frequency range of interest, $a/\lambda_0 \approx 0.29$. This structure does not support any acceptor-type modes since no holes were moved around. The only perturbation is reduction of the size of the holes, and therefore only the modes from the air band are pulled down into the bandgap due to the increased overlap with high-dielectric-constant material. Finally, integration of any kind of cavity with this type of waveguide is very easy since the full symmetry of the type 0 waveguide is preserved.

If we increase the size of holes in one row [Fig. 9(b)], we form the waveguide (type 5) that can operate in a real single-mode regime of operation. By making the holes bigger, the only modes that are localized in the line defect are acceptor-type modes. For $r_{\text{defect}} = 0.45a$ the first-order acceptor-type mode is centered around the midgap frequency and can be used for guiding of light. This mode is expected to have a higher group velocity than any of the modes described so far due to its slope in the ω–β dispersion relation. Also, the mode spans a wider fre-

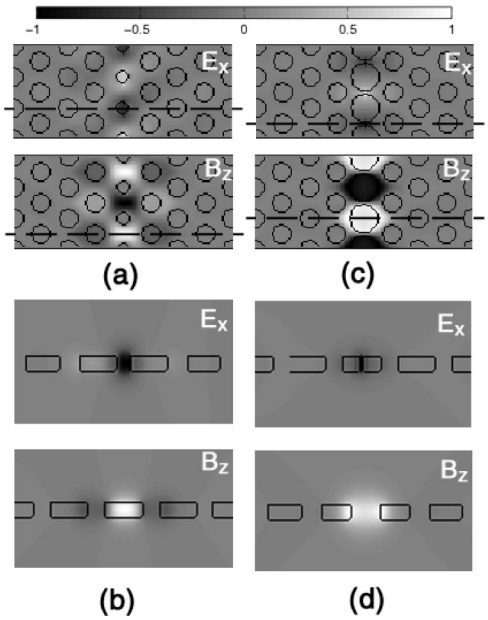

Fig. 10. (a), (b) Field patterns of mode 1 in the type 4 waveguide with $r_{\text{defect}} = 0.2a$. (c), (d) Field patterns of the guided mode in the type 5 waveguide with $r_{\text{defect}} = 0.45a$. (a) and (c) show field profiles at the middle of the slab, and (b) and (d) show field profiles at the positions indicated by dashed lines in the (a) and (c), respectively. Field patterns are shown for $\beta = \pi/a$.

quency range than any other mode. These two features are desirable to have efficient transport of energy along the waveguide. However, by increasing the size of the holes, the efficiency of turning sharp bends might decrease due to the increased vertical losses since the light is less confined to the slab (bigger holes). This feature needs to be investigated in more detail.

The type 5 waveguide is a very interesting structure for investigation of fundamental properties of the PC guiding mechanism. The reason is that modes guided in this structure are truly photonic-bandgap-effect guided modes. Guiding by effective refractive-index contrast[10] is not possible, since the "core" of the waveguide (the row with bigger holes) actually has a smaller effective refractive index than the surrounding PPC does [Fig. 9(c)]. Therefore TM-like modes will not be guided in this structure at all.

In Figs. 10(a) and 10(b) we show field patterns of mode 1 in the type 4 waveguide for $r_{\text{defect}} = 0.2a$, and in Figs. 10(c) and 10(d) we show the acceptor mode of the type 5 waveguide for $r_{\text{defect}} = 0.45a$. Both modes have odd lateral symmetry, and E_x and B_z have antinodes at the middle of the waveguide. Therefore it is possible to efficiently couple TE-polarized light into the waveguide. It is interesting to note that in the case of the type 4 waveguide the E field reaches maximum in the reduced holes [Fig. 10(a)], and in the case of the type 5 waveguide the E field reaches maximum in the dielectric regions [Fig. 10(c)]. This is because in the case of the type 4 waveguide the mode is pulled down from the air band (the E field is localized in the holes), and in the case of the type 5 waveguide the mode is pulled up from the dielectric band (the E field is localized in the dielectric), as shown in Fig. 6.

5. CONCLUSIONS

In conclusion, we have presented and analyzed in three dimensions, using the FDTD algorithm, several methods of controlling positions of guided modes within the PPC-based waveguides. The ability to engineer positions of guided modes is very important to achieve efficient guiding (reduced vertical and lateral losses), efficient coupling of light into the structure, and frequency matching of eigenmodes of coupled PC-based devices (i.e., cavities coupled to waveguides). The appearance of acceptor-type modes in donor-type waveguides is observed and explained. The importance of the relative position of holes versus the absolute amount of added high-dielectric-constant material is emphasized.

ACKNOWLEDGMENTS

The authors thank Tomoyuki Yoshie for many valuable discussions.

This research was supported by the U.S. Air Force Office of Scientific Research through contract F49620-98-1-0447 and by the National Science Foundation through contract ECS-9632937.

REFERENCES

1. E. Yablonovitch, "Inhibited spontaneous emission in solid-state physics and electronics," Phys. Rev. Lett. **58**, 2059–2062 (1987).
2. J. D. Joannopoulos, R. D. Meade, and J. N. Winn, *Photonic Crystals* (Princeton University, Princeton, NJ, 1995).
3. T. F. Krauss, R. M. De La Rue, and S. Brand, "Two-dimensional photonic-bandgap structures operating at near infrared wavelengths," Nature **383**, 692–702 (1996).
4. S. G. Johnson, S. H. Fan, P. R. Villeneuve, J. D. Joannopoulos, and L. Kolodziejski, "Guided modes in photonic crystal slabs," Phys. Rev. B **60**, 5751–5758 (1999).
5. R. D. Meade, A. Devenyi, J. D. Joannopoulos, O. L. Alerhand, D. A. Smith, and K. Kash, "Novel applications of photonic band-gap materials: low-loss bends and high Q cavities," J. Appl. Phys. **75**, 4753–4755 (1994).
6. A. Mekis, J. C. Chen, I. Kurland, S. H. Fan, P. R. Villeneuve, and J. D. Joannopoulos, "High transmission through sharp bends in photonic crystal waveguides," Phys. Rev. Lett. **77**, 3787–3790 (1996).
7. A. Chutinan and S. Noda, "Waveguides and waveguide bends in two-dimensional photonic crystal slabs," Phys. Rev. B **62**, 4488–4492 (2000).
8. S. Kuchinsky, D. C. Allen, N. F. Borelli, and J. C. Cotteverte, "3D localization in a channel waveguide in a photonic crystal with 2D periodicity," Opt. Commun. **175**, 147–152 (2000).
9. S. G. Johnson, P. R. Villeneuve, S. H. Fan, and J. D. Joannopoulos, "Linear waveguides in photonic-crystal slabs," Phys. Rev. B **62**, 8212–8222 (2000).
10. M. Lončar, T. Doll, J. Vučković, and A. Scherer, "Design and fabrication of silicon photonic crystal optical waveguides," J. Lightwave Technol. **18**, 1402–1411 (2000).
11. T. Sondergaard, A. Bjarklev, M. Kristensen, J. Erland, and J. Broeng, "Designing finite-height two-dimensional photonic crystal waveguides," Appl. Phys. Lett. **77**, 785–787 (2000).
12. M. D. B. Charlton, S. W. Roberts, and G. J. Parker, "Guided mode analysis, and fabrication of a 2-dimensional visible photonic band structure confined within a planar semiconductor waveguide," Mater. Sci. Eng., B **49**, 155–165 (1997).
13. A. Adibi, R. K. Lee, Y. Xu, A. Yariv, and A. Scherer, "Design of photonic crystal optical waveguides with singlemode propagation in the photonic bandgap," Electron. Lett. **36**, 1376–1378 (2000).
14. T. Baba, N. Fukaya, and J. Yonekura, "Observation of light propagation in photonic crystal optical waveguides with bends," Electron. Lett. **35**, 654–655 (1999).
15. M. Tokushima, H. Kosaka, A. Tomita, and H. Yamada, "Lightwave propagation through a 120° sharply bent single-line defect photonic crystal waveguide," Appl. Phys. Lett. **76**, 952–954 (2000).
16. M. Lončar, D. Nedeljković, T. Doll, J. Vučković, A. Scherer, and T. P. Pearsall, "Waveguiding in planar photonic crystals," Appl. Phys. Lett. **77**, 1937–1939 (2000).
17. S. Y. Lin, E. Chow, S. G. Johnson, and J. D. Joannopoulos, "Demonstration of highly efficient waveguiding in a photonic crystal slab at the 1.5-μm wavelength," Opt. Lett. **25**, 1297–1299 (2000).
18. A. Taflove, *Computational Electrodynamics: The Finite-Difference Time-Domain Method* (Artech House, Norwood, Mass., 1995).
19. S. H. Fan, P. R. Villeneuve, and J. D. Joannopoulos, "Large omnidirectional band gaps in metallodielectric photonic crystals," Phys. Rev. B **54**, 11245–11251 (1996).
20. Y. Xu, R. K. Lee, and A. Yariv, "Adiabatic coupling between conventional dielectric waveguides and waveguides with discrete translational symmetry," Opt. Lett. **25**, 755–757 (2000).
21. H. Benisty, "Modal analysis of optical guides with two-dimensional photonic band-gap boundaries," J. Appl. Phys. **79**, 7483–7492 (1996).